

Characterization of a High-Speed, High-Power Semiconductor Master-Oscillator Power-Amplifier (MOPA) Laser as a Free-Space Transmitter

M. W. Wright¹

Semiconductor lasers offer promise as high-speed transmitters for free-space optical communication systems. This article examines the performance of a semiconductor laser system in a master-oscillator power-amplifier (MOPA) geometry developed through a Small Business Innovation Research (SBIR) contract with SDL, Inc. The compact thermo-electric cooler (TEC) packaged device is capable of 1-W output optical power at greater than 2-Gb/s data rates and a wavelength of 960 nm. In particular, we have investigated the effects of amplified spontaneous emission on the modulation extinction ratio and bit-error rate (BER) performance. BERs of up to 10^{-9} were possible at 1.4 Gb/s; however, the modulation extinction ratio was limited to 6 dB. Other key parameters for a free-space optical transmitter, such as the electrical-optical efficiency (24 percent) and beam quality, also were measured.

I. Introduction

Free-space optical communication from near-Earth orbit requires compact, efficient, and reliable lasers that are capable of high-speed modulation at high power with good beam quality. Semiconductor diode lasers lend themselves well to this application and have been extensively developed due to the demand from the terrestrial telecommunications market [1]. Lasers for fiber-based communication systems typically are low-power devices though, so to extend the modulation performance to high-power operation, novel device structures and geometries have been investigated [2]. This includes the master-oscillator power-amplifier (MOPA) device in which output from a low-power oscillator capable of high-speed modulation is amplified in a separate tapered amplifier that maintains the good beam quality [3]. Having a discrete MOPA design allows the oscillator device structure to be optimized for speed and the amplifier optimized separately for power. Such an all-diode device is characterized in the laboratory, and the results are reported.

¹ Communications Systems and Research Section.

The research described in this publication was carried out by the Jet Propulsion Laboratory, California Institute of Technology, under a contract with the National Aeronautics and Space Administration.

II. Approach and Experiment

A discrete-diode MOPA was delivered by SDL, Inc. under a phase II Small Business Innovation Research (SBIR) contract; a schematic is shown in Fig. 1. The device lased at 960 nm with the oscillator wavelength detuned slightly from the gain peak of the amplifier. As discussed below, this was required to limit the saturated power of the amplifier and optimize the modulation performance at high output power. The packaged device involved 60 dB of isolation between the oscillator and amplifier. The collimated output from the amplifier was not isolated. The oscillator device structure was a multi-quantum-well InGaAs active-region Fabry–Perot diode in a high-speed package with up to 10 mW of fiber-coupled power available. Based on the stand-alone oscillator output power, the fiber-coupling efficiency was estimated as approximately 25 percent. The amplifier also was composed of a multi-quantum-well InGaAs structure in a broad-area diode, approximately 2 mm in length, with a tapered contact region to match the beam diffraction and preserve the beam quality during amplification. The amplifier was anti-reflection coated to limit parasitic oscillations in the device.

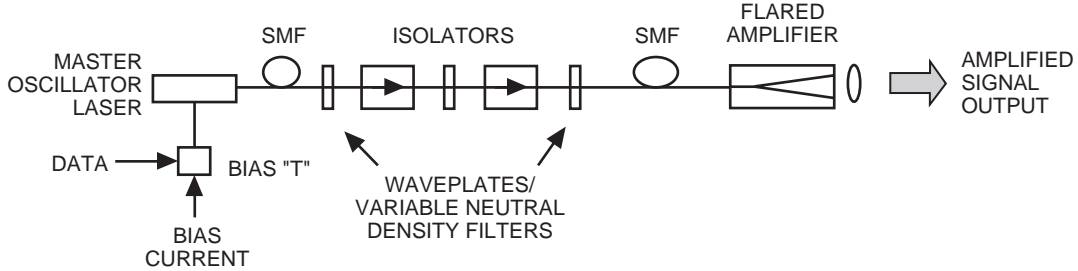


Fig. 1. The discrete-diode MOPA device. (SMF denotes single-mode fiber coupling.)

In order to fully characterize the laser and determine its applicability to free-space communication systems, several experiments were performed on the laser in continuous-wave (CW) and pulsed mode. A Micrologic bit-error rate (BER) tester was used to evaluate the BER performance up to a data rate of 1.4 Gb/s (the limit of the instrument) in non-return-to-zero (NRZ) format with variable pseudo-random bit-sequence (PRBS) word lengths from PN 7 through PN 23. A fast-pulse generator allowed eye diagrams to be obtained at up to 2.5 Gb/s to determine the degree of jitter and quality of the modulation. The diagrams were recorded on a 6-GHz sampling oscilloscope. The output from the oscillator alone could be sampled to differentiate the influence of the amplifier on the BER and jitter as well. Distortions in the bit pattern also were investigated at various current settings in order to provide insight into device anomalies. A New Focus Si photodiode with a 3-dB bandwidth of 1 GHz (corresponding to a 2-Gb/s data rate) was used as the detector. The signal could be optionally sampled through a Uniphase, Inc. clock and data recovery (CDR) unit that automatically lock onto data rates up to 2.5 Gb/s as provided by the BER tester or fast-pulse generator. Power measurements at various amplifier injection current levels were obtained to determine the effects of amplified spontaneous emission, which limits the modulation extinction ratio. Other measurements included the beam quality, the overall electrical-to-optical efficiency, and optical spectra.

III. Results and Discussion

The output power for diode lasers is depicted by a light-versus-current (LI) curve. The LI of the overall device as a function of the amplifier current is shown in Fig. 2, with the oscillator alone shown in the inset. The packaged MOPA output power was limited to 1 W because only an air-cooled thermo-electric cooler (TEC) was used. With water cooling and better anti-reflection coatings on the device, a table-top unit was able to produce 3.6 W of CW output power [4]. In normal operation, the oscillator is biased at 20 mA and a 2-V peak-to-peak rf signal is applied through an rf coupler onto the CW bias current. Applying this voltage across the 50- Ω impedance-matched termination corresponds to a ± 20 -mA modulation about the bias point. Plotting the output power as a function of the oscillator current (see Fig. 3) allows one

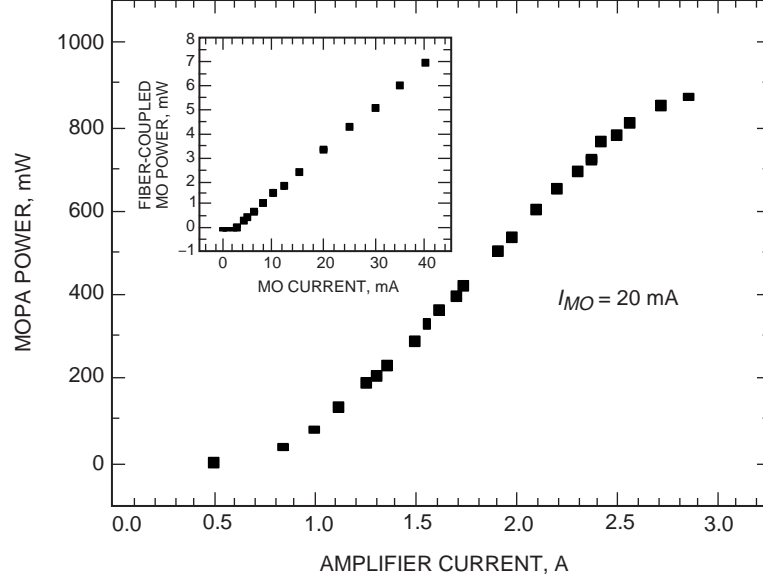


Fig. 2. The LI curve for the amplifier. The inset shows the LI curve for the master oscillator (MO) alone.

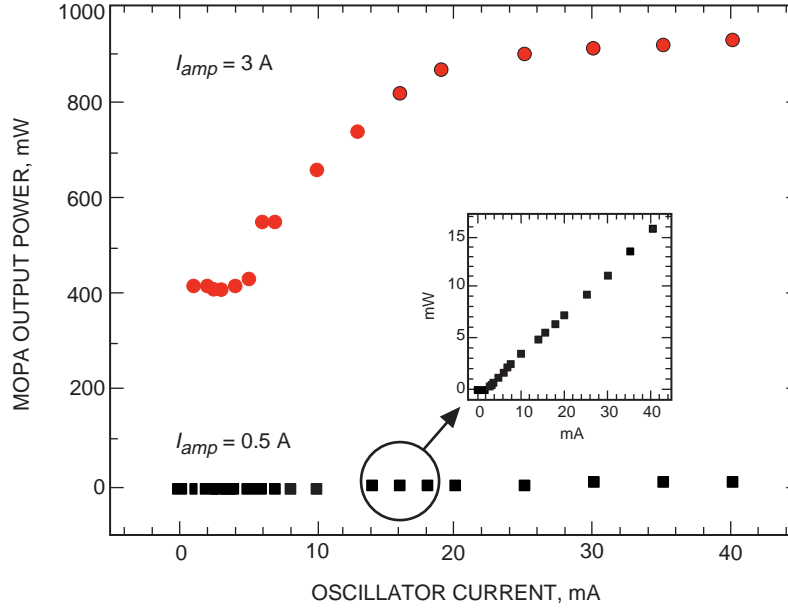


Fig. 3. The LI curve as a function of oscillator current. The inset is an enlargement of the bottom curve.

to investigate, under CW operation, the effect of the oscillator modulation on the output power. With the maximum amplifier current, $I_{amp} = 3$ A, and no oscillator current, $I_{MO} = 0$ mA, the output power still is seen to be fairly significant. This effectively corresponds to the transmission of an “off” bit when the device is operated in a pulsed mode and is due to the amplified spontaneous emission (ASE) that occurs from broad-area laser diodes. The modulation extinction ratio is limited to around 3 dB. However, most of this light is not coupled into the lasing mode and hence will diverge widely as the beam is propagated. To simulate propagation over a large distance and select only the on-axis modes, the output beam is spatially filtered through a single-mode fiber. The modulation extinction ratio, given as the ratio of output power

at maximum to minimum modulation, is seen in Fig. 4 to increase to 6 dB with the amplifier at 3.0 A. However, some ASE still is present on axis as decreasing the amplifier current to 0.5 A increases the extinction ratio to greater than 10 dB, as revealed in the Fig. 4 inset. Coupling into the single-mode fiber was not optimized for optical efficiency, as revealed by the drop in overall power. Maximum coupling of a diffraction-limited spot into a single-mode fiber can be as high as 50 to 60 percent.²

The influence of the ASE also can be seen in the optical spectrum. A low-resolution spectrum of the MOPA output with no oscillator input is shown in Fig. 5(a) from a multi-mode fiber-coupled optical spectrum analyzer. Weak lasing modes can be seen on top of the broad ASE peak, indicating the presence of the deleterious effect of facet reflections. Ideally, the amplifier is anti-reflection coated to avoid the generation of competing lasing modes. When the oscillator is turned on, Fig. 5(b), the spectrum collapses

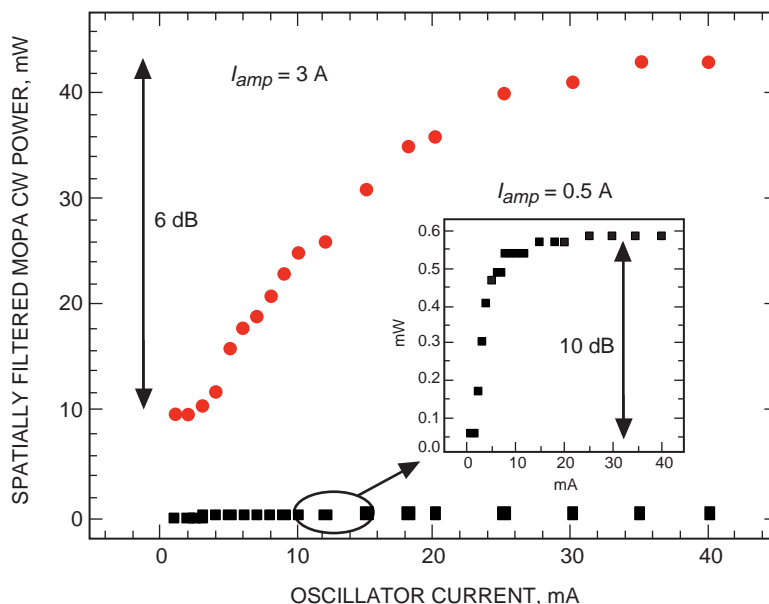


Fig. 4. The LI curve with a spatial filter from coupling through a single-mode fiber. The inset is an enlargement of the bottom curve.

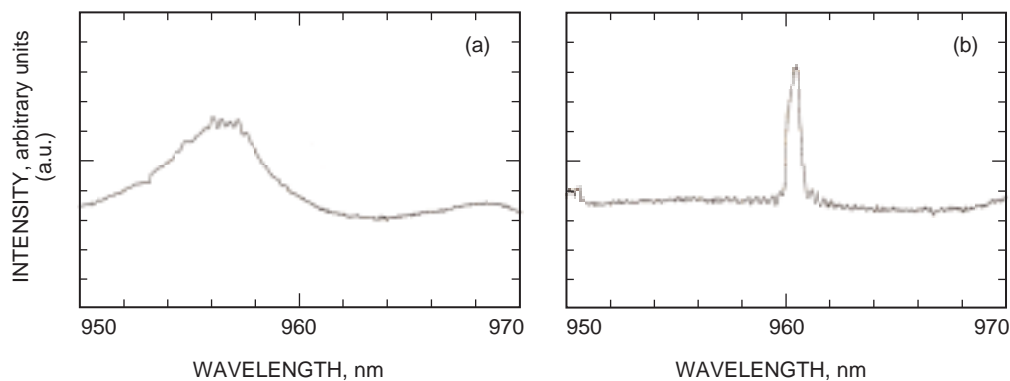


Fig. 5. Optical spectrum: (a) amplifier, $I_{amp} = 2.8\text{ A}$, $I_{MO} = 0\text{ mA}$ and (b) MOPA (with ND filter), $I_{amp} = 2.8\text{ A}$, $I_{MO} = 20\text{ mA}$.

² See, for example, Blue Sky Research, "Fiber Coupling Data Sheet," San Jose, California, 1999.

to a more typical lasing spectrum representative of the oscillator spectrum. The multi-longitudinal-mode output is unable to be resolved in this figure, even when the device is modulated. Note that the oscillator wavelength is on the low energy side of the amplifier gain peak. This was chosen in the device fabrication to reduce the unsaturated gain of the amplifier and, hence, optimize the modulation performance of the device. The 60 dB of isolation between the oscillator and the amplifier was required for a similar reason.

A bandpass filter centered at 960 nm was placed in the output beam to investigate the power level of the ASE. Figure 6(a) shows that, within the 11-nm full-width, half-maximum (FWHM) bandwidth of the filter and the 45 percent transmission efficiency, no significant decrease of the power was measured as a function of amplifier current. This would indicate that, when the amplifier gain is saturated from the oscillator, most of the effect of the ASE power is as a spatially divergent wavefront with a narrow spectral width. When the amplifier gain is unsaturated, at the lower oscillator currents shown in Fig. 6(b), the filtered power is significantly less than the filter transmission. This suggests that the majority of the amplifier ASE at low oscillator current is outside of the 11-nm bandwidth centered on the 960-nm lasing wavelength.

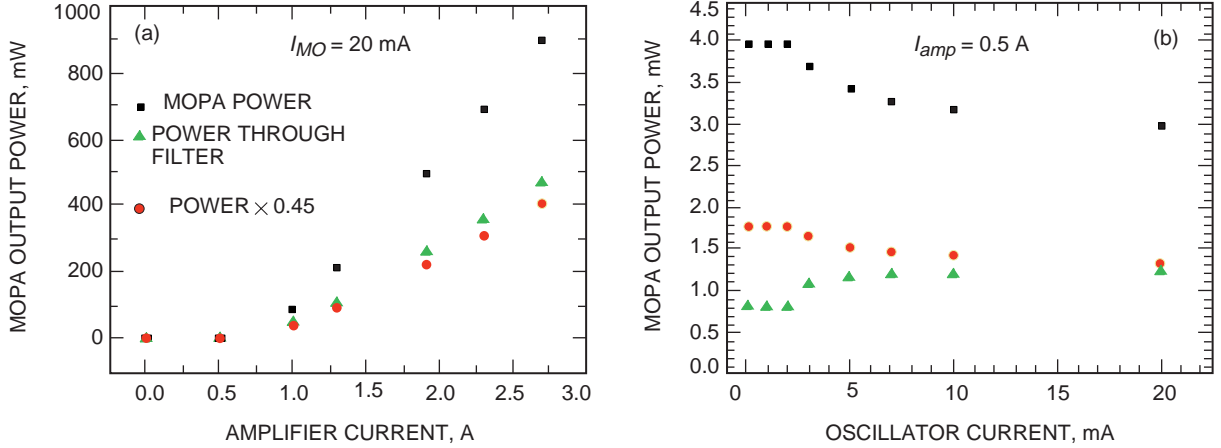


Fig. 6. The CW MOPA LI curves with narrow bandpass filter: (a) as a function of amplifier current and (b) as a function of oscillator current. When the amplifier is saturated, $I_{MO} = 20 \text{ mA}$, the ASE is negligible, as shown by the overlap of the filtered power and the filter transmissivity (45 percent). At low oscillator and amplifier currents, spectrally broad ASE becomes dominant.

Before leaving the power measurements, it is worth noting the overall efficiency of the MOPA device. Since the oscillator consumes relatively little current as compared with the amplifier, the efficiency is calculated as the product of the current and the voltage drop across the amplifier, as plotted in Fig. 7 as a function of amplifier current. The required TEC power also has been included, but it is only of the order of 1 percent as compared with the amplifier power requirement. The peak efficiency of around 24 percent is obtained at greater than 0.8 W of output power. This compares to approximately 40 to 50 percent for typical broad-area laser diodes [5] and is lower due to the current losses incurred by the tapered amplifier design used to maintain the high beam quality.

Eye diagrams are a convenient way to characterize the modulation performance of laser sources for optical communication systems. The scatter in the upper and lower states represents the noise in each bit, and the crossover scatter represents the jitter. Both of these figures of merit impact the overall quality of the eye opening and, hence, the modulation. As mentioned above, the modulation performance is affected by the level of unsaturated gain in the amplifier, which is determined by the strength of the oscillator input to the amplifier. If the operating level of the oscillator is altered, then the oscillator signal strength can be adjusted by varying the wave plates in the setup while maintaining the isolation. Unless noted, the following data were taken for an optimized oscillator current value of 20 mA.

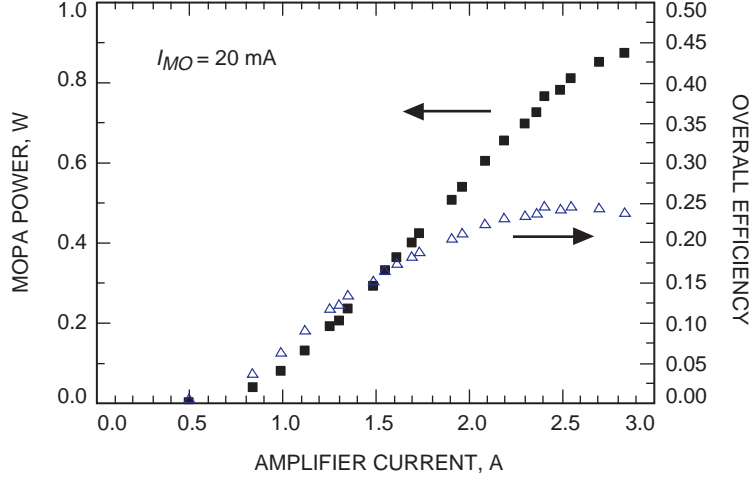


Fig. 7. Overall electrical-optical efficiency.

Figure 8 shows the first set of eye diagrams, taken from the oscillator alone by splitting off the signal prior to injection into the amplifier. The pseudo-random bit-sequence (PRBS) non-return-to-zero (NRZ) data rate was varied from 500 Mb/s to 2.5 Gb/s, Figs. 8(a) through 8(e). The maximum rate the CDR unit was able to lock onto was around 2 Gb/s, Fig. 8(f), due to the increase in jitter above that rate. However, the retimed data reveal good fidelity compared with the rf input signal at 2.5 GHz shown in Fig. 8(g). A representative bit pattern is shown in Fig. 9(a) with the corresponding eye diagram in Fig. 9(b). Most of the bit noise appears to be due to the ringing from the leading edge of the pulse, either in the 0 or 1 bit. Varying the depth of modulation from 0.5 V to 2 V peak-to-peak did not alter the noise significantly.

The modulation of the entire MOPA output is shown in Fig. 10(a) through 10(e), with the amplifier set at the maximum of 3 A to give nearly 1 W of output power. Several ND filters were placed in the beam to limit the power incident on the detector. At the data rate of 2.5 Gb/s, the output is severely degraded with significant noise and jitter present. However, clock and data recovery were again possible up to 2 Gb/s, as shown in Fig. 10(e). The influence of the amplifier ASE on the modulation is again shown in the eye diagrams of Fig. 11. As the amplifier current is increased, the jitter remains approximately the same, but the noise in the off state is increased. The absolute scale cannot be compared due to the inclusion of ND filters. The cause of the increased noise can be more clearly determined by comparing eye diagrams resulting from the transmission of distorted bit patterns. These were obtained by altering the modulation voltage and the oscillator bias current value to a nonoptimal setting. An example is shown in Fig. 12. The dominant effect in this case is caused by overshoot and ringing of the pulses. The large overshoot arises from the transition from the off to the on state and causes isolated 1 bits to have a higher value than a sequences of 1's. Similarly, there exists an undershoot on the transition to an off state. Ringing following the leading bit edge then increases the noise in each state, deforming the eye opening. The overshoot is intrinsic to optical amplifiers, where the gain builds up during the oscillator off state and is accentuated in semiconductor devices due to the fast carrier lifetimes [6]. Several features already have been included in the design of the device that mitigate the effect of the overshoot, but evidently undershoot and ringing on the transition to 0 still are present in the amplifier and produce significant noise in the off state at high power. These features include injecting the amplifier on the low energy side of the gain peak and attenuating the oscillator injected signal. From the LI curves, it can be seen that the amplifier is well saturated at the higher oscillator currents, so introducing loss reduces the gain saturation and, hence, the overshoot without a significant sacrifice in output power. An additional electronic option would involve having an adjustable decision point in the detection circuitry.

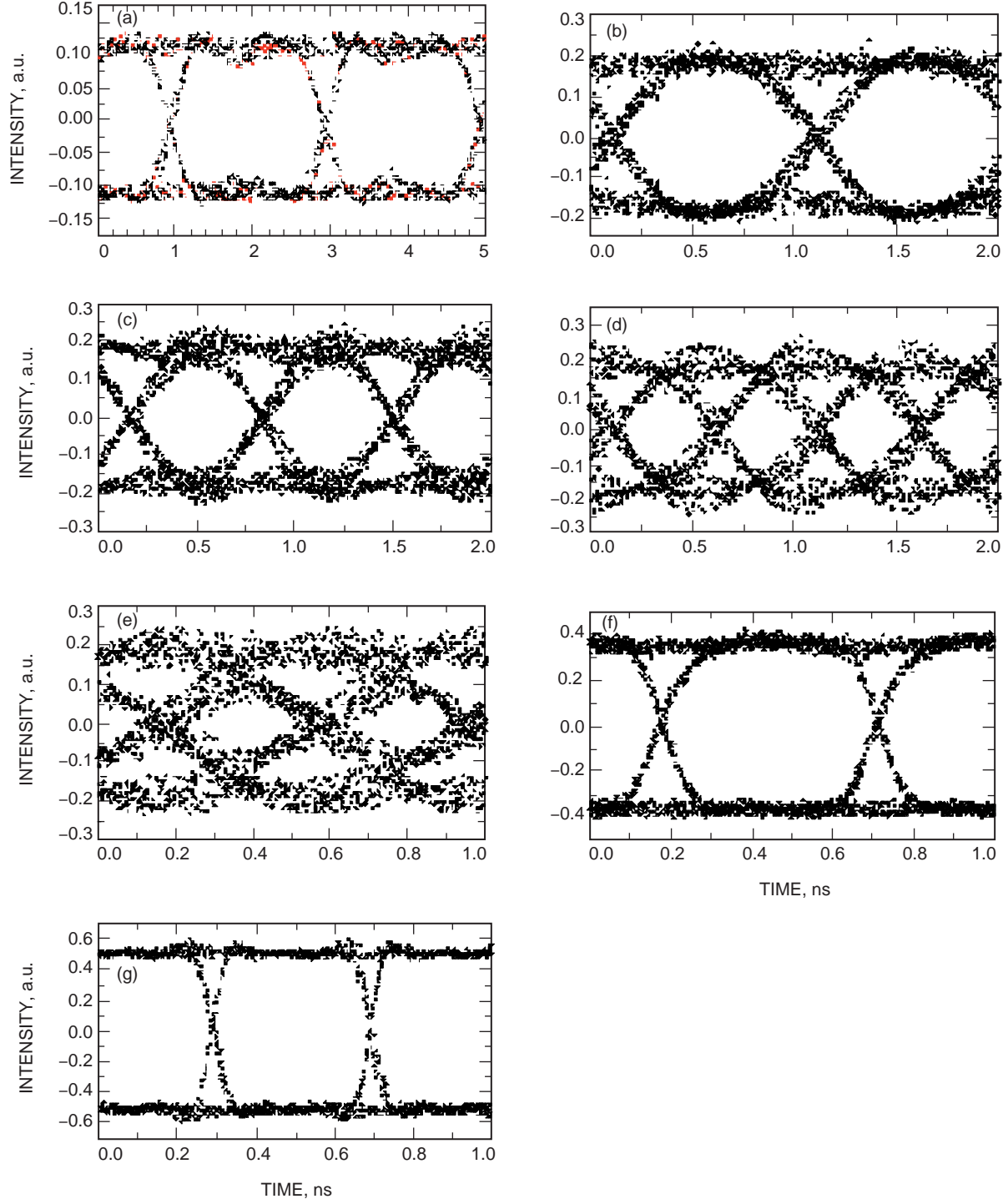


Fig. 8. Oscillator eye diagrams for data rates of (a) 500 Mb/s, (b) 1 Gb/s, (c) 1.5 Gb/s, (d) 2.0 Gb/s, (e) 2.5 Gb/s, (f) 1.9 Gb/s after CDR, and (g) the rf input signal, 2.5 Gb/s. ($I_{MO} = 20$ mA, PRBS, NRZ, $2V_{p-p}$ modulation.)

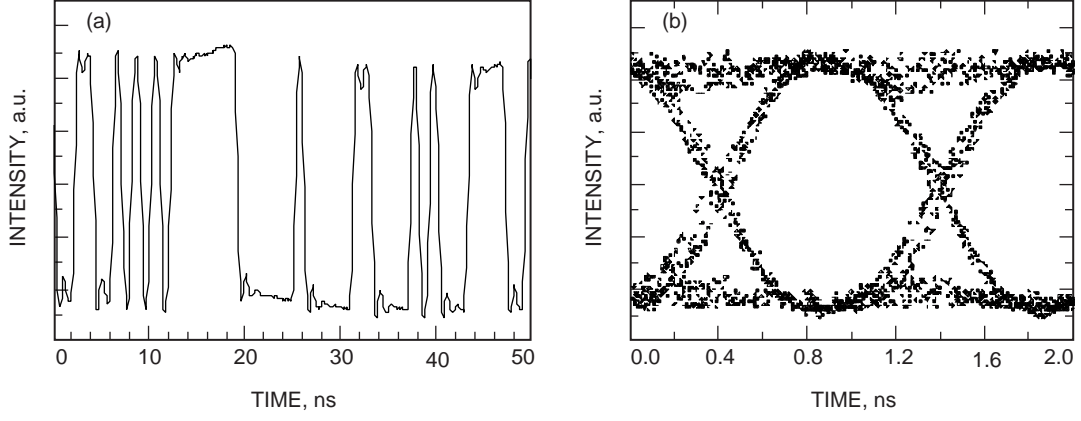


Fig. 9. Oscillator (a) bit pattern and (b) eye diagram ($I_{MO} = 20$ mA, 1 Gb/s, $2 V_{p-p}$ modulation).

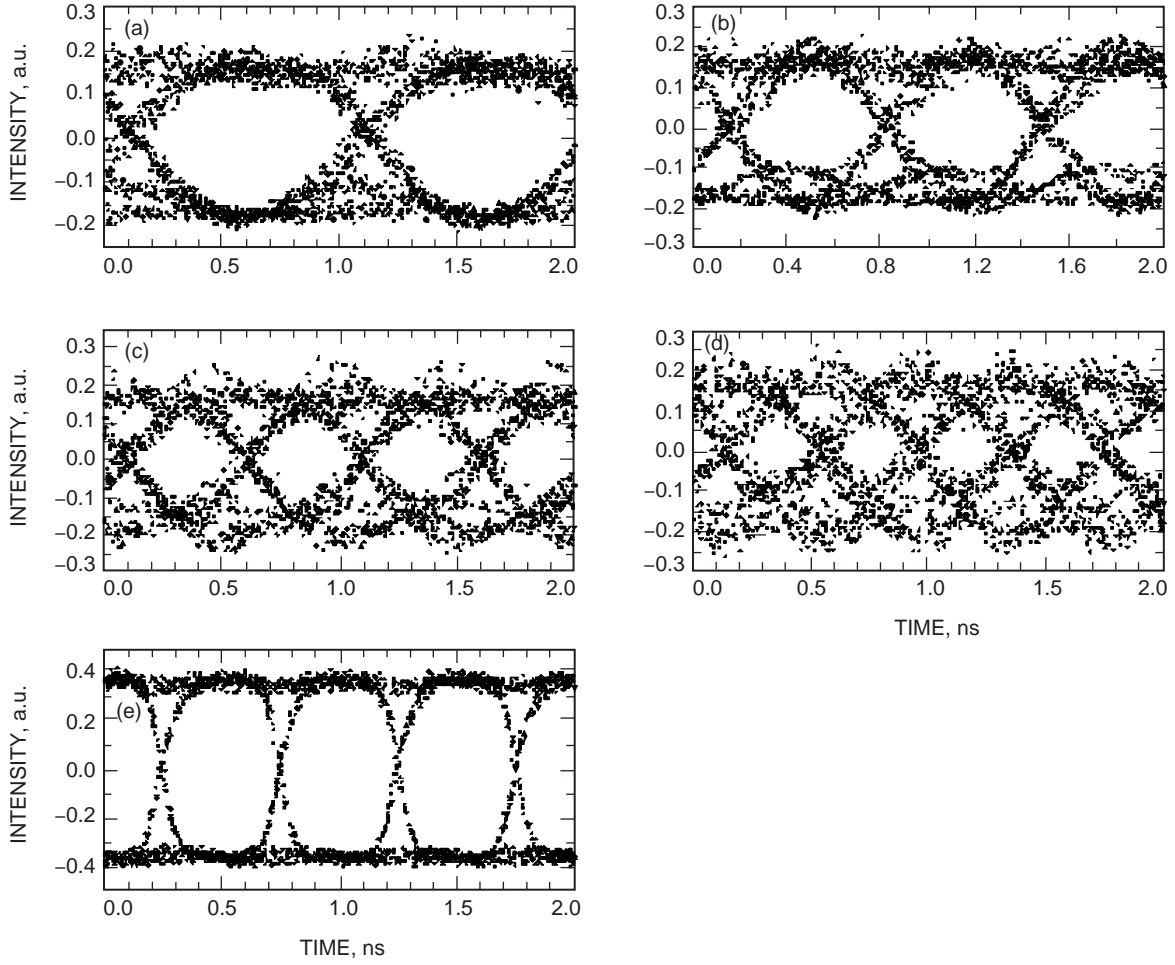


Fig. 10. MOPA eye diagrams for data rates of (a) 1.0 Gb/s, (b) 1.5 Gb/s, (c) 2.0 Gb/s, (d) 2.5 Gb/s, and (e) 2.0 Gb/s after CDR. ($I_{MO} = 20$ mA, $I_{amp} = 3$ A, $2 V_{p-p}$ modulation, PRBS, NRZ.)

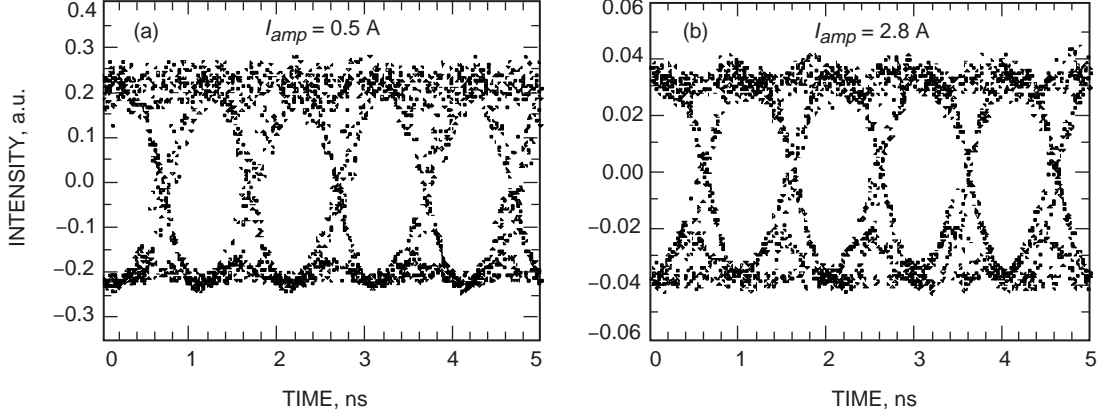


Fig. 11. MOPA eye diagrams: $I_{MO} = 20$ mA, 1 Gb/s, and amplifier current at (a) minimum and (b) maximum.

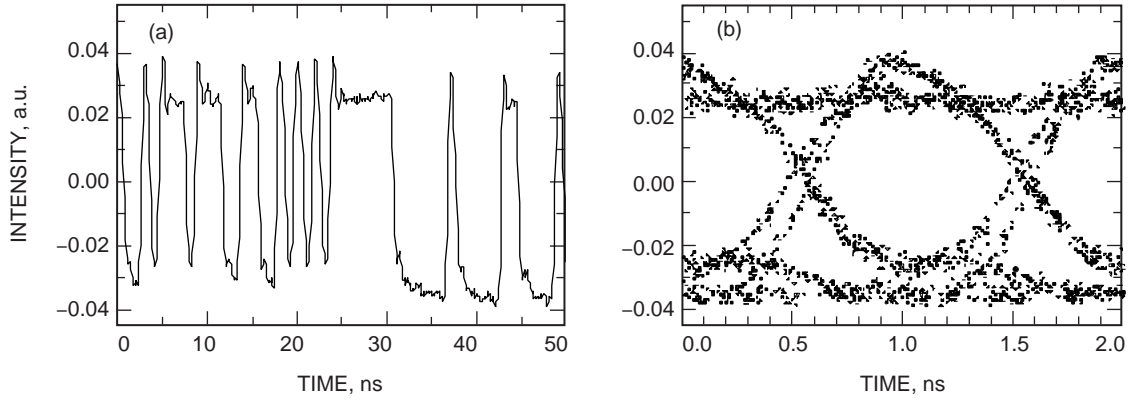


Fig. 12. Distorted (a) bit pattern and (b) eye diagram for MOPA ($I_{MO} = 22.72$ mA, $I_{amp} = 2.8$ A, 1 Gb/s, 2 V_{p-p} modulation).

The BER measurements give a quantitative measure of the overall system performance in a communication link [7]. The received power was calculated from the gain and responsivity of the detector and from measuring the dc and ac voltages as the optical signal was varied. The detector used was not optimized for high sensitivity at low signal levels since, for a laboratory-based device, detecting the signal is not an issue. The received power levels then could be improved with the choice of a more sensitive detector. Determining the performance of the laser as a data transmitter is still relevant though, especially at the amplified signal levels. The BER is plotted in Fig. 13 as a function of received power by placing a variable ND filter in the beam and focusing the output onto the photodiode. The amplified signal shows some scatter, but the general monotonic decrease in BER with increasing power is evident. An approximate 5-dB penalty occurs as compared with the BER from the output of the oscillator alone, as well as a reduction in the noise on the data. However, when the MOPA output is spatially filtered, the original oscillator BER is obtained with indications of a slight 1-dB improvement. This is consistent with the degradation observed in the amplifier eye diagram and reflects the improvement in the modulation extinction ratio when the ASE is filtered out. A sample eye diagram also is shown in the inset of Fig. 13 at the higher BER prior to loss of synchronization.

The device beam quality was not examined in detail because the device had a collimation optic integrated at the output. If one were to examine the amplifier output directly, the beam would be seen to be very astigmatic due to the amplifier geometry and output dimensions. However, correcting optics are used to give a collimated elliptical beam with close to diffraction-limited beam quality as determined from

similar amplifier characterizations.³ Figure 14 shows a representative mode pattern near the 1-W power level with the oscillator modulated around 20 mA. The side peak is an artifact of the measuring system and is due to scattering from the multiple ND filters required to limit the intensity incident on the camera. With the amplifier at transparency, the beam is much more elliptical due to the predominance of ASE at these lower amplifier current levels. The polarization of the amplifier output beam is TE polarized, parallel to the plane of the growth. In an application, light propagated through the atmosphere and the receiver optical system experiences varying levels of transmission based on the polarization of the beam. Hence, the beam should be converted to circular polarization by a $\lambda/4$ wave plate to optimize the transmission along a free-space optical path.

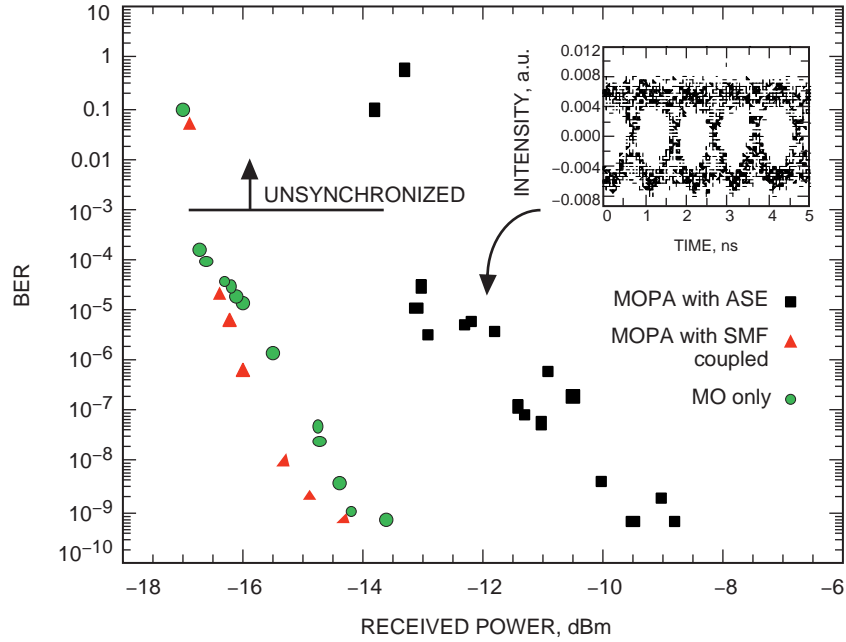


Fig. 13. BER for MOPA, MOPA with a spatial filter (SMF), and MO alone ($I_{MO} = 20$ mA, $I_{amp} = 2.8$ A, 2 V_{p-p} modulation, 1.4 Gb/s PN 7 data with CDR).

IV. Conclusion

A discrete MOPA semiconductor diode laser built by SDL, Inc. was characterized as a high-power, high-speed transmitter for free-space optical communications. Synchronization of data rates up to 2 Gb/s was possible at near 1-W output power and a wavelength of 960 nm. The modulation extinction ratio was limited to 6 dB due to the effects of ASE. This could be improved without a sacrifice in output power, as a similar water-cooled table-top device has been shown to give an extinction ratio of as large as 13 dB. The main difference is the material and anti-reflection coating quality of the amplifier. Eye diagrams reveal good modulation, and BERs up to 10^{-9} were possible at 1.4 Gb/s using PN 7-coded PRBS data at a -14 dBm received signal. The received power is limited by the sensitivity of the detector used in the setup. The overall device efficiency, including the TEC, peaked at 24 percent with 0.8 W of output power. In summary, the compactness of the all-diode approach shows good promise as a MOPA transmitter for free-space optical communications, but the performance needs to be improved, specifically the modulation extinction ratio and efficiency, to compare with a fiber-based amplifier system that has also reached commercialization [8].

³ SDL, Inc., personal communication, San Jose, California, February 1999.

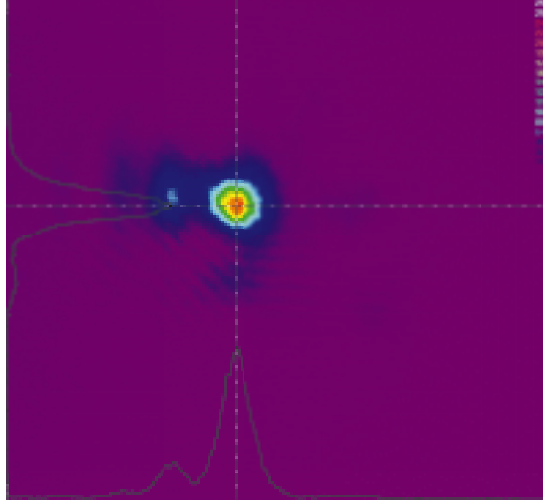


Fig. 14. CW MOPA mode pattern
 $(I_{MO} = 20 \text{ mA}, I_{amp} = 2.8 \text{ A})$.

References

- [1] G. P. Agrawal and N. K. Dutta, *Semiconductor Lasers*, 2nd ed., New York: Van Nostrand Reinhold, 1993.
- [2] J. N. Walpole, "Semiconductor Amplifiers and Lasers with Tapered Gain Regions," *Opt. Quant. Elect.*, vol. 28, no. 6, pp. 623–645, 1996.
- [3] R. Park, D. F. Welch, A. Hardy, R. Lang, D. McHays, S. O'Brien, K. Dzurko, and D. Scifres, "2 W CW, Diffraction Limited Operation of a Monolithically Integrated Master Oscillator Power Amplifier," *IEEE Photon. Tech. Lett.*, vol. 5, no. 3, pp. 297–300, 1993.
- [4] E. C. Vail, M. Hagberg, S. O'Brien, M. Ziari, and R. Lang, "Demonstration of 2.5 Gb/s at 3.6 W Using a Semiconductor Flared Optical Amplifier," *IEEE International Conference on Semiconductor Lasers*, Nara, Japan, 1998.
- [5] J. G. Endriz, M. Vakili, G. S. Browder, M. DeVito, J. M. Haden, G. L. Harne-gal, W. E. Plano, M. Sakamoto, D. F. Welch, S. Willing, D. P. Worland, and H. C. Yao, "High Power Diode Laser Arrays," *IEEE J. Quant. Elect.*, vol. 28, no. 4, pp. 952–965, 1992.
- [6] H. Ghafouri-Shiraz, *Fundamentals of Laser Diode Amplifiers*, New York: John Wiley and Sons, 1996.
- [7] E. Desurvire, *Erbium Doped Fiber Amplifiers*, New York: John Wiley and Sons, 1994.
- [8] G. E. Tourgee, Lucent Technologies, Press Release, July 1999.